Environ. Sci. Technol. **2003**, *37,* 5424−5431

Hydroformylation of 1-Hexene in Supercritical Carbon Dioxide: Characterization, Activity, and Regioselectivity Studies

ANNE E. MARTEEL,[†] TIMOTHY T. TACK,[‡] SELMA BEKTESEVIC,[‡] JULIAN A. DAVIES,[†] MARK R. MASON,[†] AND MARTIN A. ABRAHAM*[,‡]

Department of Chemistry and Department of Chemical and Environmental Engineering, The University of Toledo, Toledo, Ohio 43606

The hydroformylation of alkenes is a major commercial process used for the production of oxygenated organic compounds. When the hydroformylation reaction is performed using a homogeneous catalyst, an organic or aqueous solvent is employed, and a significant effort must be expended to recover the catalyst so it can be recycled. Development of a selective heterogeneous catalyst would allow simplification of the process design in an integrated system that minimizes waste generation. Recent studies have shown that supercritical carbon dioxide ($scCO_2$) as a reaction solvent offers optimal environmental performance and presents advantages for ease of product separation. In particular, we have considered the conversion of 1-hexene to heptanal using rhodium- and platinum-phosphine catalysts tethered to supports insoluble in $scCO_2$ to demonstrate the advantages and to understand the limitations of a solid-catalyzed process. One of the historical limitations of supported catalysts is the inability to control product regioselectivity. To address this concern, we have developed tethered catalysts with phosphinated silica and controlled pore size MCM-41 and MCM-20 supports that provide improved regioselectivity and conversion relative to their nonporous equivalents. Platinum catalysts supported on MCM-type supports were the most regioselective whereas the analogous rhodium catalysts were the most active for hydroformylation of 1-hexene in $scCO_2$.

Introduction

Homogeneous hydroformylation reactions using rhodium-phosphine catalysts in organic solvents have been extensively studied and reviewed (*1*−*3*). It is well-known that an important problem with homogeneous catalysts is the difficulty to recover and recycle these catalysts. To eliminate the need for the separation and recovery steps, heterogeneous catalysis involving supported catalysts can be used. This improves the environmental performance of the process by eliminating the use of organic solvents and the energy consumption associated with the recovery process.

Organic polymeric (*4*−*7*) and inorganic supports have been studied for heterogeneous catalysis (*8*−*11*). Inorganic supports such as silica are more mechanically stable and resistant against aging and solvent attack relative to their polymeric analogues. However, the impregnation technique that is often used to prepare silica-supported rhodium catalysts has generally resulted in high levels of rhodium leaching and poor activity and selectivity.

An alternative to impregnation is the use of sol−gel condensation to prepare phosphinated silica supports (*12*−*15*). The incorporation of the metal complex can then be accomplished by stirring a mixture of the metal complex and the phosphinated support in aqueous ethanol under nitrogen. This synthesis enables a stronger coordination of the metal complex to the phosphinated support, decreasing considerably the leaching of rhodium. To improve the selectivity of heterogeneous catalysts, the use of MCM mesoporous molecular sieves as supports has been considered (*11*, *16*). The MCM supports are attractive because they provide easy separation of the catalyst from organic species and high turnover numbers. The synthesis of micelle-templated silicas based on the neutral templating method (*17*) offers many advantages such as the simple washing for separation and the easy recovery and reuse of the template, which enhances the "greenness" of the manufacture of the catalysts.

Although it has been well-documented that homogeneous platinum/tin systems are efficient for hydroformylation and especially asymmetric hydroformylation, only a few studies have been performed using heterogeneous platinum/tin systems (*18*, *19*). The conversion of silica-supported platinum catalysts was usually low with high rates of hydrogenation and isomerization. Supported platinum catalysts have not previously been studied as hydroformylation catalysts in $scCO_2$, aside from our recently communicated preliminary results (*20*).

Because of its environmental advantages, the use of $scCO_2$ as a replacement for organic solvents in chemical reactions has been widely investigated. Carbon dioxide is nontoxic, does not form air-polluting daughter products, and additionally, is cheap and plentiful. Work on hydroformylation in $scCO_2$ has been ongoing since Rathke et al. (*21*) first reported on hydroformylation of propene by cobalt. Investigators have attempted to develop effective homogeneous hydroformylation catalysts that are soluble in $scCO_2$ and also provide sufficient activity and selectivity to be commercially viable (*22*−*25*). In nearly all cases, the activity was comparable to that obtained in liquid-phase reactions, and reasonable selectivity (typically L/B = 2−3) was obtained.

In the present work, the combination of the advantages of using catalysts supported on inorganic materials prepared via an environmentally preferable synthesis and the use of the environmentally benign solvent $scCO_2$ is studied. The synthesis and characterization of silica- and MCM-supported rhodium and platinum catalysts is described. The hydroformylation results are presented in terms of activity and regio- and chemoselectivity to demonstrate the value of using MCM supports for selective hydroformylation chemistry.

Experimental Section

Phosphinated silica support **1a** (*14*) and siliceous MCM-41 (support **1b**) and MCM-20 (support **1c**) were prepared as previously reported (*16*). The preparation of phosphinated MCM-41 and MCM-20 supports followed the procedure described by Bemi et al. for modification of silica (*26*).

* Corresponding author phone: (419)530-7391; fax: (419)530-7392; e-mail: martin.abraham@utoledo.edu.
[†] Department of Chemistry.
[‡] Department of Chemical and Environmental Engineering.

10.1021/es034544n CCC: $25.00
Published on Web 10/22/2003

TABLE 1. Summary of the Different Supports and Supported Metal Catalysts

support	support no.	metal precursor	catalyst no.
phosphinated silica	**1a**	$[RhCl(1,5\text{-cod})]_2$	**4a**
phosphinated MCM-41	**1b**	$[RhCl(1,5\text{-cod})]_2$	**4b**
phosphinated MCM-20	**1c**	$[RhCl(1,5\text{-cod})]_2$	**4c**
phosphinated silica	**1a**	$PtCl_2\{Ph_2P(CH_2)_2Si(OEt)_3\}_2$	**7a**
phosphinated MCM-41	**1b**	$PtCl_2\{Ph_2P(CH_2)_2Si(OEt)_3\}_2$	**7b**
phosphinated MCM-20	**1c**	$PtCl_2\{Ph_2P(CH_2)_2Si(OEt)_3\}_2$	**7c**

The rhodium precursor $[RhCl(1,5\text{-cod})]_2$ (cod = cyclooctadiene) was synthesized as previously reported (*27*). Rhodium catalysts supported on phosphinated silica supports were prepared in our laboratory using procedures described elsewhere (*13*, *14*). Rhodium catalyst supported on MCM-41 (catalyst **4b**) was prepared by stirring $[RhCl(1,5\text{-cod})]_2$ (0.05 g; 0.11 mmol) in 100 mL of ethanol for 15 min, after which the phosphinated MCM-41 support **1b** (1.00 g; 0.44 mmol of P) was added, and the mixture was stirred for 24 h under nitrogen. The product was isolated by filtration under nitrogen, and the yellow catalyst was dried under vacuum overnight. The phosphinated MCM-20-supported rhodium catalyst **4c** was synthesized with the phosphinated MCM-20 support **1c** following the same procedure described for catalyst **4b** except that 81.6 mg of $[RhCl(1,5\text{-cod})]_2$ and 1.40 g of support **1c** were used. The platinum precursor $PtCl_2\{Ph_2P(CH_2)_2Si(OEt)_3\}_2$ (*26*), phosphinated silica-supported platinum catalyst **7a**, and phosphinated MCM-41-supported platinum catalyst **7b** were prepared as previously reported (*20*). Phosphinated MCM-20-supported platinum catalyst **7c** was prepared following the same procedure as that for catalyst **7b**. All the catalysts have a metal to phosphorus molar ratio of 1:2. Table 1 summarizes the different supports, metal precursors, and catalysts used in this work.

Silica (**1a**) and MCM-type (**1b**, **1c**) supports, silica- and MCM-supported rhodium catalysts (**4a**−**4c**), and supported platinum catalysts (**7a**−**7c**) were characterized using CP/MAS ^{13}C and ^{31}P NMR spectroscopy. All the catalysts were characterized after hydroformylation using elemental analysis and CP/MAS ^{13}C and ^{31}P NMR spectroscopy and are named "used" catalysts.

All NMR solution spectra were recorded on a Varian VXR-400 spectrometer at 25 °C. Frequencies and standards were as follows: $^{31}P\{^1H\}$ NMR: 161.9 MHz, external standard 85% H_3PO_4/D_2O; ^1H NMR: 400 MHz, standard tetramethylsilane (TMS); $^{13}C\{^1H\}$ NMR: 100.4 MHz, standard TMS. The solid-state CP/MAS NMR spectra were recorded on a Chemagnetics M200-S spectrometer operating at 4.7 T. The CP/MAS NMR spectra were all obtained using cross-polarization (CP), magic angle spinning (MAS), and high-power proton decoupling. Frequencies and standards: ^{13}C NMR: 50.2 MHz, standard hexamethylbenzene; ^{31}P NMR: 80.8 MHz, standard triphenylphosphine (PPh_3). The uncertainties in chemical shifts and coupling constants are estimated to be ±1 ppm and ±50 Hz, respectively, for the CP/MAS measurements. Errors in reported line width are estimated to be 10%.

Elemental analyses were carried out by Schwarzkopf Microanalytical Laboratory (Woodside, NY). A duplicate analysis was performed for each sample. Duplicate BET surface area measurements were performed using a Micromeritics AutoChem 2910 volumetric adsorption analyzer.

The procedure for the hydroformylation reactions in $scCO_2$ using supported rhodium catalysts has been previously published (*13*−*15*). The hydroformylation reactions using supported platinum catalysts were performed in a similar manner except that the addition of a co-catalyst $SnCl_2{\cdot}2H_2O$ is necessary to obtain reasonable yields. A platinum to tin molar ratio of 1:3.5 was used when performing hydroformylation with catalysts **7a**−**7c**.

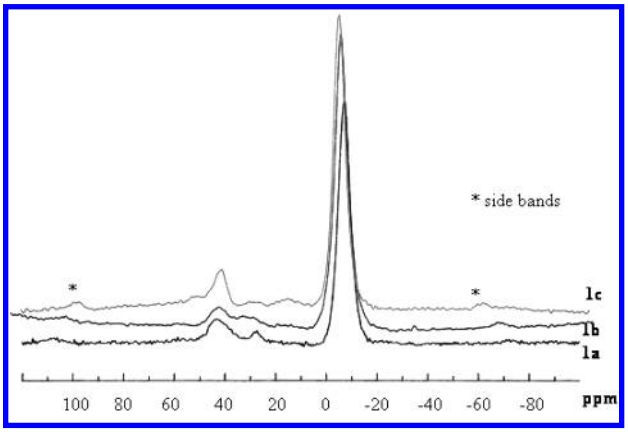

FIGURE 1. CP/MAS ^{31}P NMR spectra of phosphinated silica support 1a, MCM-41 support 1b, and MCM-20 support 1c.

Results and Discussion

Substantial catalyst characterization was conducted and is described here. Following the discussion of the catalyst materials, results obtained from the use of these catalysts for the hydroformylation of 1-hexene are presented.

Catalyst Characterization. As the modified supports were insoluble in common laboratory solvents, CP/MAS ^{31}P and ^{13}C NMR spectroscopy were the preferred techniques for characterization. The CP/MAS ^{31}P NMR spectra of phosphinated supports **1a**−**1c** are shown in Figure 1 and revealed resonances near 43.5 and −8 ppm; the asterisks indicate spinning sidebands in the spectra. By comparison with the solution ^{31}P NMR of the ligand used in the preparation of the supports, the resonance near −8 ppm was determined to be a result of supported, uncoordinated phosphine. The presence of the deshielded resonance near 43.5 ppm was indicative of a phosphorus(V) species as observed in the CP/MAS ^{31}P NMR spectrum of oxidized support **1a**. Support **1b** exhibited a low-intensity resonance at 28 ppm that has not been assigned, although we speculate that it may be due to an additional phosphorus(V) species.

The CP/MAS ^{13}C NMR spectra of supports **1a**−**1c** are shown in Figure 2 and reveal several peaks: at 130 ppm (C_6H_5-), centered at 60 ppm (-CH_2-O-), and centered around 20 ppm (-CH_2-Si- and -CH_2-P-). The assignment of the resonances reported in this work is in agreement with those reported by Komoroski et al. (*28*).

The CP/MAS ^{13}C NMR spectrum of the rhodium precursor $[RhCl(1,5\text{-cod})]_2$ revealed two resonances with the same intensity: one centered at 30 ppm (allylic carbons) and the other centered around 80 ppm (vinylic carbons). The platinum precursor $PtCl_2\{Ph_2P(CH_2)_2Si(OEt)_3\}_2$ was characterized as previously described (*26*).

Catalysts **4a**−**4c** were characterized using CP/MAS ^{31}P NMR spectroscopy before hydroformylation, as shown in Figure 3. Two resonances around 40 and −10 ppm were observed for catalyst **4a**. The resonance at −10 ppm accounted for the presence of uncoordinated phosphorus, and the one at 40 ppm represented species with Rh−P couplings and/or the presence of oxidized phosphorus

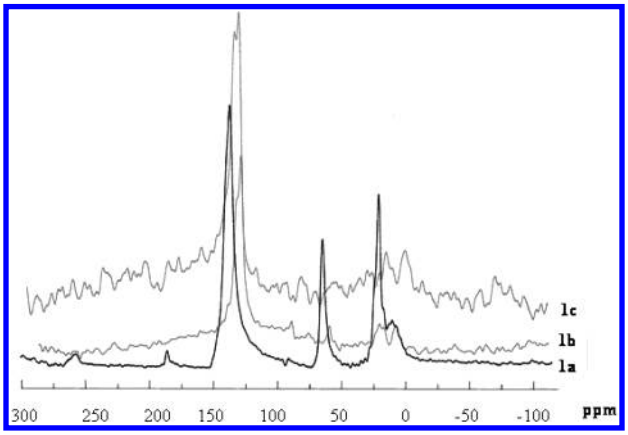

FIGURE 2. CP/MAS ^{13}C NMR spectra of phosphinated silica support 1a, MCM-41 support 1b, and MCM-20 support 1c.

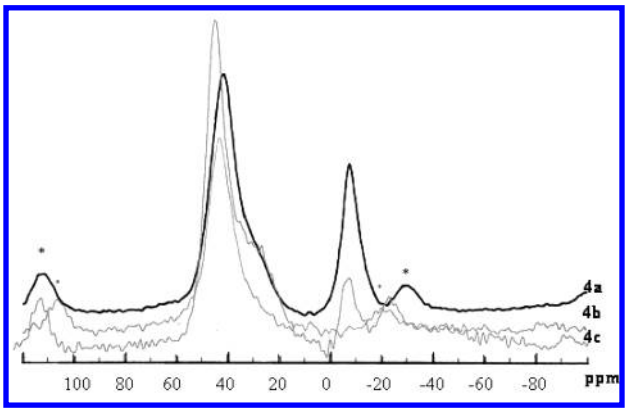

FIGURE 3. CP/MAS ^{31}P NMR spectra of fresh rhodium catalysts supported on silica (4a), MCM-41 (4b), and MCM-20 (4c).

species. In contrast, the CP/MAS ^{31}P NMR spectra of catalysts **4b** and **4c** before hydroformylation presented only a broad resonance centered at 42 ppm. There is no uncoordinated phosphorus evident in the CP/MAS ^{31}P NMR spectra of the catalysts with MCM-41 supports. A possible explanation might be the difference in the synthesis of supports on silica and on MCM-41. The formation of silica by hydrolysis of tetraethoxysilane and the condensation reaction with the phosphine ligand were performed in one step, likely leading to some diphenylphosphino moieties that were inaccessible to the metal complex. In contrast, the preparation of the phosphinated MCM-41 support was via attachment of the ligand to the surface of preformed MCM-41, resulting in a support in which all diphenylphosphino moieties were accessible to the metal complex and the absence of uncoordinated phosphine.

TABLE 2. BET Surface Areas of Catalysts Synthesized in This Project

catalyst	BET surface area (m^2/g)	catalyst	BET surface area (m^2/g)
4a	8.60; 9.16	**7a**	250.2; 252.4
4b	642.1; 651.7	**7b**	715.6; 708.3
4c	829.5; 856.8	**7c**	645.9; 654.2

In the CP/MAS ^{13}C NMR spectra of catalysts **4a**−**4c**, the ethene spacer is characterized by broad peaks around 30 ppm. The comparison between the CP/MAS ^{13}C NMR spectrum of $[RhCl(1,5\text{-cod})]_2$ and the CP/MAS ^{13}C NMR spectra of rhodium catalysts revealed that they exhibited the features of both the cyclooctadiene (resonances at 30 and 80 ppm) and the support **1a** (resonances at 130 and 60 ppm). The CP/MAS ^{13}C NMR spectra of catalysts **4b** and **4c** revealed that the majority of the features in the CP/MAS ^{13}C NMR spectra of these catalysts corresponded to those of the phosphinated MCM-41 support **1b**.

The CP/MAS ^{31}P NMR spectra of catalysts **7a**−**7c** all exhibited a single resonance associated with $^1J(^{195}Pt-^{31}P)$ of 3634 Hz (at 12 ppm), 3567 Hz (at 13 ppm), and 3701 Hz (at 12 ppm), respectively, as shown in Figure 4. The value of the line width at half-height for catalyst **7a** is 1010 Hz and is 969 Hz for catalyst **7b**, which provides evidence of the distorted environment of the immobilized platinum complexes. The symmetry of the central resonances suggests that only one type of phosphorus species is present. It has to be noted that there was no phosphorus(V) species present in the CP/MAS ^{31}P NMR spectra of the immobilized platinum complexes. Furthermore, the value of the coupling constant corresponding to the mixture of *cis*- and *trans*-$PtCl_2\{Ph_2P(CH_2)_2Si(OEt)_3\}_2$ complexes on silica gel and on MCM-41 demonstrates that the geometry of the complex $PtCl_2\{Ph_2P(CH_2)_2Si(OEt)_3\}_2$ switched to a cis geometry when the platinum complex is anchored on the surface of these supports. It is thought that a cis conformation would favor the attachment of the phosphorus species to the support.

The BET surface areas of all the different metal catalysts are presented in Table 2. The comparison of the BET surface

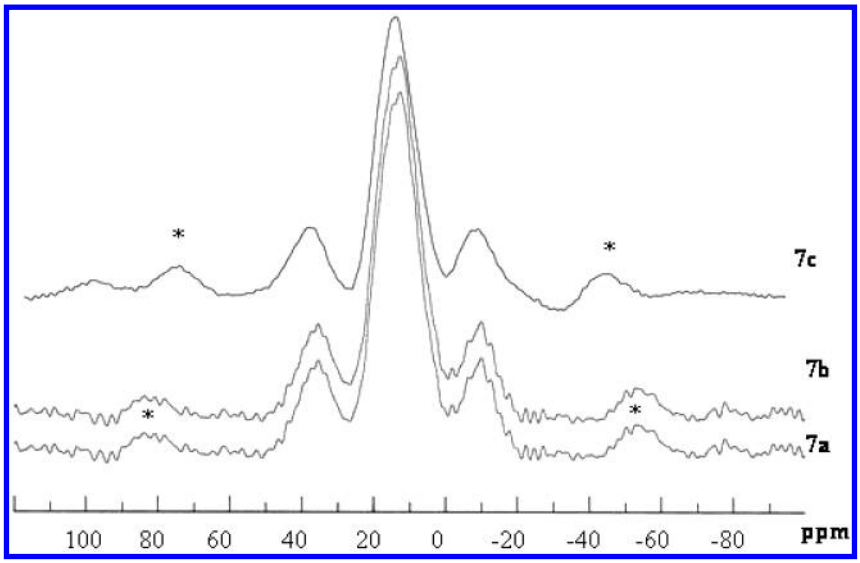

FIGURE 4. CP/MAS ^{31}P NMR spectra of platinum/tin catalysts supported on silica (7a), MCM-41 (7b), and MCM-20 (7c).

TABLE 3. Elemental Analysis of Catalysts after One Hydroformylation Reaction[a]

catalyst (molar metal: P ratio = 1:2)	wt % of phosphorus measd	wt % of metal measd	calcd molar metal:P ratios range
4a	2.91; 2.88	3.78; 4.59	0.39−0.48
used **4a**	2.72; 2.77	3.40; 3.40	0.37−0.38
4b	0.95; 0.91	1.84; 1.81	0.57−0.61
used **4b**	0.76; *	0.60; *	0.24
4c	1.20; 1.21	1.81; 1.82	0.45−0.46
used **4c**	1.01; *	1.01; *	0.30
7a	0.90; 0.86	2.61;*	0.46−0.48
used **7a**	1.52; 2.13; 2.29	0.54; 0.71; 0.76	0.31−0.67
7b	1.66; 1.69	4.91; 4.83	0.45−0.47
used **7b**	1.62; *	0.095; *	0.0093
7c	1.62; 1.79	4.43; 4.36	0.39−0.43
used **7c**	0.52; 0.63	3.44; 3.49	0.867−1.065

[a] An asterisk (*) indicates insufficient sample for duplicate analysis.

areas (S_{BET}) of the different rhodium complexes anchored on phosphinated silica, MCM-41, and MCM-20 shows the following trend: S_{BET} catalyst **4a** < S_{BET} catalyst **4b** < S_{BET} catalyst **4c**. The surface area of these catalysts represents the total surface of the samples in contact with the external environment and corresponds to the summation of the internal surface of the pores plus the external surface of the particles. As expected, catalysts prepared on supports with small pores provided the largest surface area. The comparison of the BET surface areas of catalysts **7a** and **7b** showed the same trend already observed with the rhodium catalysts **4a**−**4c**. However, catalyst **7c** presented a smaller BET surface area than catalyst **7b**, which does not follow the previous trend.

Catalysts were also characterized by elemental analysis before and after hydroformylation, and the results are shown in Table 3. The elemental analysis of reused catalyst **4a** revealed a wt % P in the range 2.22−2.28 and a wt % Rh in the range 2.49−3.04. The calculated molar Rh:P ratio range was 0.33−0.41. The elemental analysis of used catalysts **4b** and **4c** revealed a loss of more than half the content of rhodium initially measured. The loss of phosphorus was about 20% of the initial weight of phosphorus measured and was less pronounced than the loss of rhodium. Catalyst **4c** anchored on MCM-20 lost less rhodium than catalyst **4b** anchored on MCM-41. The elemental analysis of used catalyst **7a** shows that the weight percent of phosphorus actually increased after hydroformylation whereas the weight percent of Pt dramatically dropped by a factor of almost 4. The increase in the wt % P after hydroformylation was also observed with rhodium catalysts. Used catalyst **7b** retained approximately the same amount of wt % P but lost almost all its Pt, resulting in a very low calculated molar Pt:P ratio following reaction. On the contrary, used catalyst **7c** had less loss of phosphorus and platinum.

The large loss of rhodium and phosphorus is a concern for reuse of the catalyst; however, this aspect was not specifically addressed in the current research. Nevertheless, previous data (*13*) indicated that there was no loss of activity for repeated experiments using the same catalyst material, for rhodium complex supported on silica materials. This result is consistent with our current hypothesis that some unreacted phosphine reagent was adsorbed onto the support, not chemically tethered, which was simply extracted from the support during the catalytic reaction. Similarly, rhodium could have complexed to some of this "unattached" phosphine to form complexes that could also have been extracted from the support under reaction conditions.

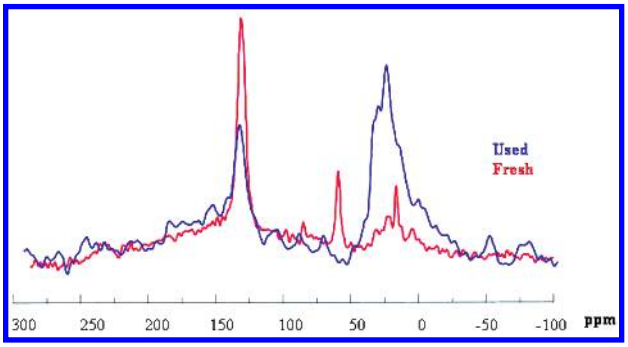

FIGURE 5. CP/MAS ^{13}C NMR spectra of used rhodium catalyst supported on MCM-41 (4b) as compared with the fresh material.

Used catalysts **4a**−**4c** were characterized by CP/MAS ^{31}P and CP/MAS ^{13}C NMR spectroscopy. The CP/MAS ^{31}P NMR spectrum revealed only one broad peak centered around 40 ppm, no different than observed for fresh catalyst. This demonstrates that there was no uncoordinated supported phosphine after hydroformylation. The broad resonance suggests the presence of different species with Rh−P couplings and/or the presence of oxidized phosphorus species.

The CP/MAS ^{13}C NMR spectra of fresh and used catalysts **4a** had the same appearance except that the peak at 80 ppm accounting for the presence of vinylic carbons of the cyclooctadiene was absent in the CP/MAS ^{13}C NMR spectrum of used catalyst **4a**. This is as anticipated since cyclooctadiene will be displaced from the rhodium during formation of the catalytically active $Rh(H)(CO)_x(PPh_2CH_2CH_2\text{-})_y$ species under reaction conditions.

Although the CP/MAS ^{13}C NMR spectra of fresh and used catalysts **4a** were similar, the CP/MAS ^{13}C NMR spectra of fresh and used catalysts **4b** and **4c** were significantly different (see Figure 5). Used catalysts **4b** and **4c** presented an unusual broad resonance between 10 and 50 ppm. This broad resonance may be due to the presence of organic species (such as heptanal) trapped in the pores of MCM-41 and MCM-20, respectively. Solid-state CP/MAS ^{13}C NMR studies were performed to characterize this broad peak. Catalyst **4b** was treated with heptanal, and a CP/MAS ^{13}C NMR spectrum was acquired. The broad peaks between 10 and 50 ppm observed in the CP/MAS ^{13}C NMR spectra of the used catalyst **4b** and catalyst **4b** treated with heptanal are identical, which is consistent with the presence of heptanal trapped within the pores of the used catalysts anchored on MCM-41. The presence of a significant amount of heptanal product in the used catalyst may partially account for the decreases in the weight percent of phosphorus and metal relative to the fresh catalyst. No attempts were made to desorb any materials from used catalysts.

The CP/MAS ^{31}P NMR spectrum of used platinum−tin catalysts **7a**−**7c** provided confirmation of the results obtained from the rhodium complex materials. The spectrum from used catalyst **7a** was substantially similar to that obtained from the fresh material. However, the spectrum from used catalysts **7b** and **7c** revealed a single broad resonance between 10 and 50 ppm, which is again consistent with the presence of adsorbed heptanal in the catalyst pores. The observance of the same peak broadening following reaction with the rhodium complex and the platinum/tin catalyst provides further evidence that the peak broadening is a result of interactions between the reactants (or products) and the catalyst support.

Reaction Analysis. Figure 6 shows the typical progress of 1-hexene hydroformylation catalyzed by a supported rhodium catalyst. The 1-hexene concentration decreases as the hydroformylation products 2-ethylpentanal, 2-methylhexa-

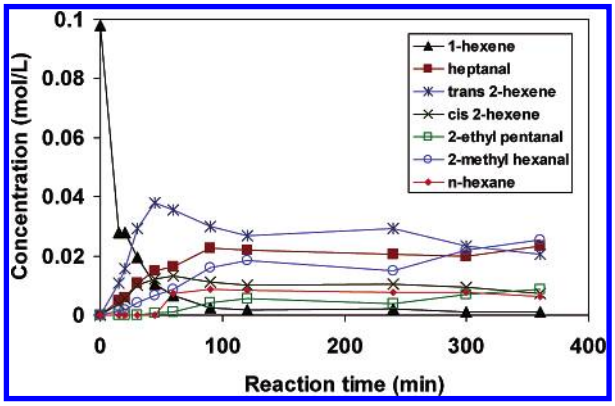

FIGURE 6. Typical reaction concentration as a function of time for rhodium catalysts on phosphinated silica and MCM-41 at 184 atm, 100 °C, $[1\text{-hexene}]_0 = 0.097$ M, $[CO]_0 = [H_2]_0 = 0.7$ M.

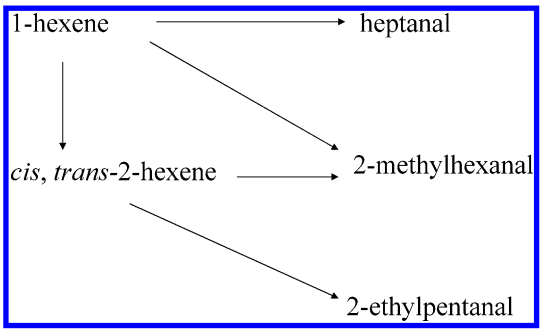

FIGURE 7. Reaction network demonstrating the pathways for the hydroformylation of 1-hexene.

nal, and heptanal increase. The isomerization products, *trans*-2-hexene and *cis*-2-hexene, eventually achieve a maximum concentration, which declines as the reaction proceeds. The hydrogenation product *n*-hexane behaves in the same manner as the isomerization products. 1-Heptanol was never observed in any of the experimental runs for any of the catalysts evaluated. All samples taken prior to 30 min are believed to reflect a brief nonhomogeneous condition in the reactor due to the addition of 1-hexene and have been observed previously (*13*, *14*). Subsequent samples taken after 30 min demonstrate a smooth decline in the concentration of 1-hexene.

Figure 7 provides a reaction pathway description for the observed product profile, which has been used previously to describe the hydroformylation of 1-hexene by supported rhodium catalysts in $scCO_2$. The reaction network shows that hydroformylation of 1-hexene produces both heptanal (the desired product), 2-methylhexanal, and isomerization products *cis*- and *trans*-2-hexene. The internal olefins can subsequently be converted to 2-ethylpentanal and 2-methylhexanal but cannot directly produce the desired heptanal product. Regioselectivity (or L/B) is defined according to these pathways as the formation of heptanal relative to the formation of the branched aldehydes, and chemoselectivity is defined as the formation of all aldehydes relative to the isomerization products.

The effect of support pore size was investigated by comparing rhodium catalysts supported on phosphinated silica, MCM-41, and MCM-20. In all cases, the temperature was maintained at 100 °C, the initial concentration of 1-hexene was 0.097 M, and the syngas ratio was 7:1 relative to the substrate. Figure 8a compares the normalized yield, and Figure 8b compares the regioselectivity of hydroformylation of 1-hexene with rhodium supported on phosphinated silica, MCM-41, and MCM-20. The yields were normalized to the mass of rhodium in order to eliminate fluctuations due to variation of rhodium concentration in experimental runs. The rhodium catalyst supported on phosphinated MCM-20 provided a greater aldehyde yield than that supported on MCM-41, which was in turn greater than the aldehyde yield obtained when the catalyst was supported on phosphinated silica. Since the surface area is greatest for MCM-20-type catalysts, it is possible that improved yield was simply due to higher surface area in the support, which might lead to better distribution of the rhodium catalyst. Measurement of rhodium "dispersion" using the hydrogen uptake method indicates that dispersion increases in the order of rhodium on phosphinated silica < rhodium on MCM-41 < rhodium on MCM-20. Greater availability of rhodium on the surface of the catalyst support could provide the observed increase in the normalized aldehyde yield.

In addition to increased aldehyde yield, higher regioselectivity was obtained by decreasing the average pore size of the support. The rhodium supported on phosphinated MCM-20 provided the highest regioselectivity. It is likely that the small pore size of the MCM-20 support provides a reaction cavity that is not desirable for formation of the branched aldehyde, leading to the increased selectivity (*29*).

Chemoselectivity, which was previously defined as the ratio of aldehyde products to the isomerization products, was also investigated and is shown in Figure 8c for the rhodium catalysts. Initially, chemoselectivity was less than 0.5, indicating that more isomerization than hydroformylation products were obtained. However, the chemoselectivity increased over time as the internal olefins were slowly converted to aldehyde products. Since the internal olefin cannot produce the linear aldehyde, the increasing chemoselectivity is accompanied by a decrease in the regioselectivity, as more branched aldehydes are produced.

In addition to rhodium catalysts on mesoporous supports, platinum/tin catalysts on mesoporous supports were also investigated. Figure 9a compares the normalized yield, and Figure 9b compares the regioselectivity of hydroformylation of 1-hexene with platinum/tin catalysts on phosphinated silica, MCM-41, and MCM-20. The platinum/tin on phosphinated MCM-20 support shows the highest normalized yield, followed by the platinum/tin catalyst on phosphinated MCM-41, which is slightly higher than that of the phosphinated silica-supported platinum/tin system. It is believed that catalysts anchored on mesoporous supports are more active than the analogous catalysts anchored on silica supports because of the increased surface area of the support.

The regioselectivity of the platinum/tin catalyst supported on phosphinated MCM-20 was the highest observed in all of the current experiments, followed by platinum on MCM-41 and silica, respectively. This suggests that the formation of linear aldehyde is enhanced relative to the formation of branched aldehydes by the decreasing pore size of the support. It is thought that the shape selectivity induced by use of a smaller average pore size causes preferential formation of the less bulky linear product.

As observed from Figures 8a and 9a, the yields obtained from the rhodium catalysts were greater than that obtained from the platinum/tin catalysts by a full order of magnitude. However, in both cases, catalysts prepared on supports with smaller average pore size provided greater aldehyde yields. Figures 8b and 9b show that platinum/tin catalysts are generally more regioselective, but that decreasing the average pore size of the support always increased the regioselectivity of the catalyst.

Figure 9c compares the chemoselectivity of platinum/tin catalyst on phosphinated silica, MCM-41, and MCM-20. In the case of the platinum/tin catalyst system, the initial chemoselectivity was near 1 and did not change substantially

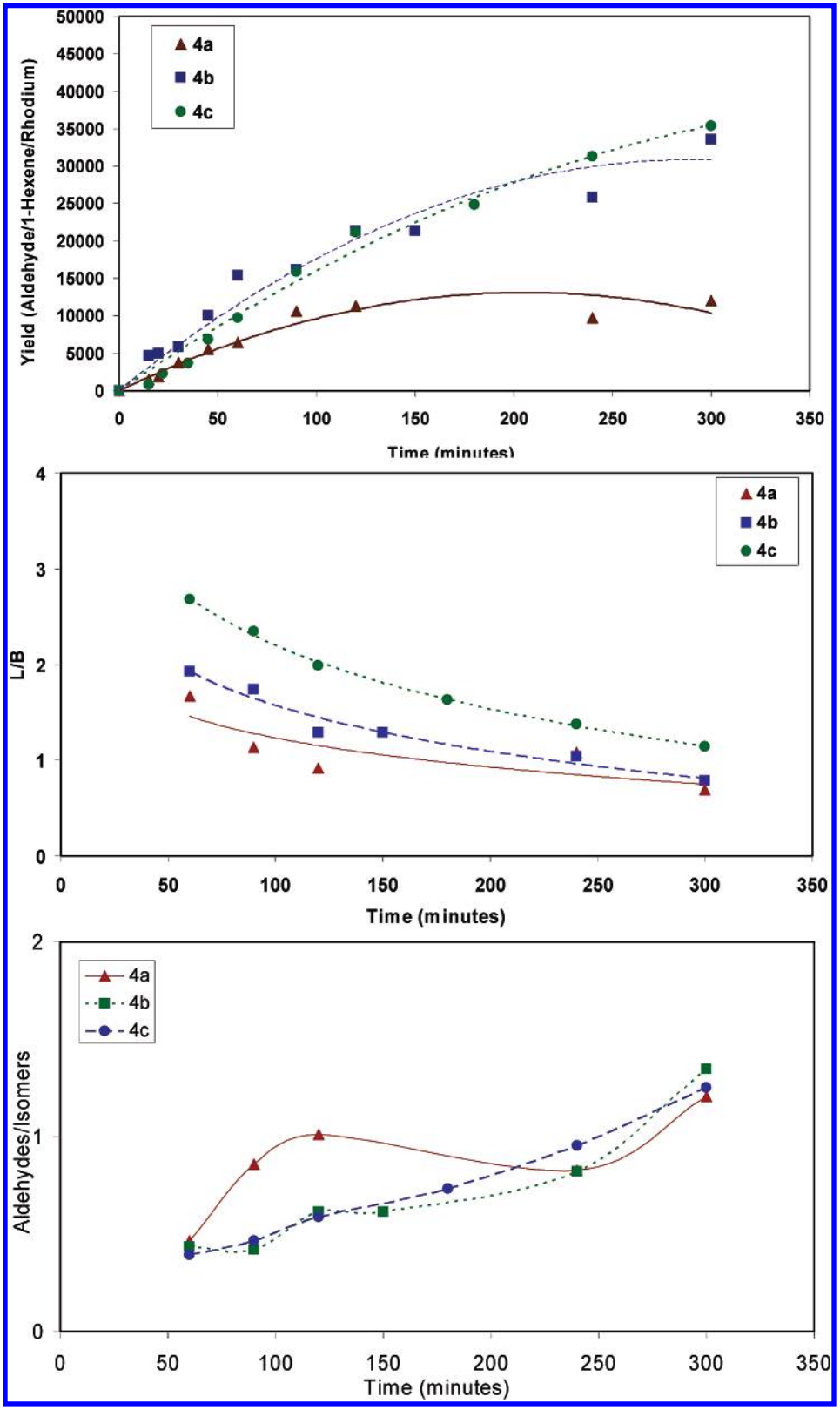

FIGURE 8. (a) Comparison of yield as a function of time for rhodium catalysts (normalized to mass of rhodium) on phosphinated silica, MCM-41, and MCM-20 at 184 atm, 100 °C, $[1\text{-hexene}]_0 = 0.097$ M, $[CO]_0 = [H_2]_0 = 0.7$ M. (b) Comparison of regioselectivity as a function of time of rhodium catalysts on phosphinated silica, MCM-41, and MCM-20 at 184 atm, 100 °C, $[1\text{-hexene}]_0 = 0.097$ M, $[CO]_0 = [H_2]_0 = 0.7$ M. (c) Comparison of chemoselectivity as a function of time for rhodium catalysts on phosphinated silica, MCM-41, and MCM-20 at 184 atm, 100 °C, $[1\text{-hexene}]_0 = 0.097$ M, $[CO]_0 = [H_2]_0 = 0.7$ M.

over time. Thus, less isomerization products are produced from the platinum/tin catalyst than were produced using the rhodium-supported materials.

In addition, it is noted that the regioselectivity obtained with the platinum/tin catalyst system was essentially constant throughout the reaction. On the basis of the pathways shown

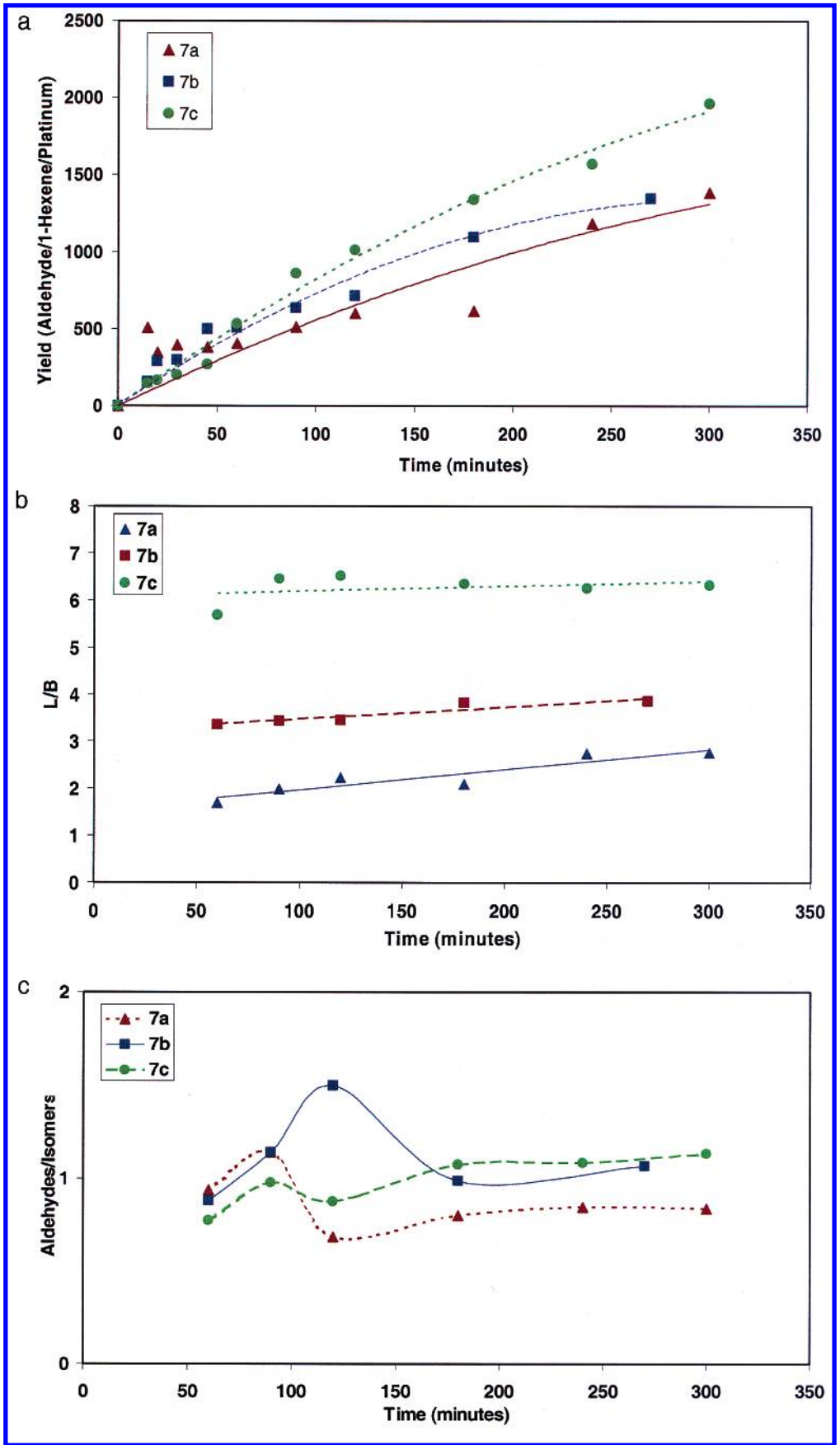

FIGURE 9. (a) Comparison of yield as a function of time for platinum/tin catalyst systems (normalized to the mass of platinum) on phosphinated silica, MCM-41, and MCM-20 at 184 atm, 100 °C, $[1\text{-hexene}]_0 = 0.097$ M, $[CO]_0 = [H_2]_0 = 0.7$ M. (b) Comparison of regioselectivity as a function of time of platinum/tin catalyst systems on phosphinated silica, MCM-41, and MCM-20 at 184 atm, 100 °C, $[1\text{-hexene}]_0 = 0.097$ M, $[CO]_0 = [H_2]_0 = 0.7$ M. (c) Comparison of chemoselectivity as a function of time of platinum/tin catalyst systems on phosphinated silica, MCM-41, and MCM-20 at 184 atm, 100 °C, $[1\text{-hexene}]_0 = 0.097$ M, $[CO]_0 = [H_2]_0 = 0.7$ M.

previously, it is thus possible to conclude that the platinum/tin catalyst is less effective in converting the internal olefin to aldehyde product, just as we have already observed the decreased activity for the platinum/tin catalyst for hydroformylation of the terminal olefin relative to the rhodium system. Thus, we conclude that the highest selectivity to the desired linear aldehyde can be obtained through the use of mesoporous MCM-20-supported platinum/tin catalysts, although rhodium catalyst supported on mesoporous MCM-20 provides reasonable selectivity with the highest yield.

Acknowledgments

Although the research described in this paper was supported by the Environmental Protection Agency under Grant R-82820601-0, it has not been subjected to the Agency's review and therefore does not necessarily reflect the views of the Agency, thus no endorsement of this research is implied. We also recognize the support of the PQ Corporation for donation of sodium silicate and Dr. Yong-Wah Kim for assistance with solid-state NMR spectroscopy.

Literature Cited

(1) Beller, M.; Cornils, B.; Frohning, C. D.; Kohlpaintner, C. W. *J. Mol. Catal. A* **1995**, *104*, 17−85.
(2) Trzeciak, A. M.; Ziółkowski, J. J. *Coord. Chem. Rev.* **1999**, *190*−*192*, 883−900.
(3) Van Leeuwen, P. W. N. M., Claver, C., Eds. *Rhodium Catalyzed Hydroformylation*, 1st ed.; Kluwer Academic Publishers: Boston, MA, 2000.
(4) Leadbeater, N. E.; Marco, M. *Chem. Rev.* **2002**, *102*, 3217−3274.
(5) McNamara, C. A.; Dixon, M. J.; Bradley, M. *Chem. Rev.* **2002**, *102*, 3275−3300.
(6) Nozaki, K.; Itoi, Y.; Shibahara, F.; Shirakawa, E.; Ohta, T.; Takaya, H.; Hiyama, T. *J. Am. Chem. Soc.* **1998**, *120*, 4051−4052.
(7) Ajjou, A. N.; Alper, H. *J. Am. Chem. Soc.* **1998**, *120*, 1466−1468.
(8) Hanaoka, T.; Arakawa, H.; Matsuzaki, T.; Sugi, Y.; Kanno, K.; Abe, Y. *Catal. Today* **2000**, *58*, 271−280.
(9) Song, C. E.; Lee, S. *Chem. Rev.* **2002**, *102*, 3495−3524.
(10) Wight, A. P.; Davis, M. E. *Chem. Rev.* **2002**, *102*, 3589−3614.
(11) De Vos, D. E.; Dams, M.; Sels, B. F.; Jacobs, P. A. *Chem. Rev.* **2002**, *102*, 3615−3640.
(12) Lu, Z.; Lindner, E.; Mayer, H. A. *Chem. Rev.* **2002**, *102*, 3543−3578.
(13) Tadd, A. R.; Marteel, A. E.; Mason, M. R.; Davies, J. A.; Abraham, M. A. *Ind. Eng. Chem. Res.* **2002**, *41*, 4514−4522.
(14) Tadd, A. R.; Marteel, A. E.; Mason, M. R.; Davies, J. A.; Abraham, M. A. *J. Supercrit. Fluids* **2003**, *25*, 183−196.
(15) Hemminger, O.; Marteel, A. E.; Mason, M. R.; Davies, J. A.; Tadd, A. R.; Abraham, M. A. *Green Chem.* **2002**, *4*, 507−512.
(16) Beck, J. S.; Vartuli, J. C.; Roth, W. J.; Leonowicz, M. E.; Kresge, C. T.; Schmitt, K. D.; Chu, C. T. W.; Olson, D. H.; Sheppard, E. W.; McCullen, S. B.; Higgins, J. B.; Schlenker, J. L. *J. Am. Chem. Soc.* **1992**, *114*, 10834−10843.
(17) Tanev, P. T.; Pinnavaia, T. J. *Science* **1995**, *267*, 865−867.
(18) Homs, N.; Clos, N.; Muller, G.; Sales, J.; de la Piscina, P. R. *J. Mol. Catal.* **1992**, *74*, 401−408.
(19) Guo, I.; Hanson, B. E.; Toth, I.; Davis, M. E. *J. Mol. Catal.* **1991**, *70*, 363−368.
(20) Marteel, A. E.; Davies, J. A.; Mason, M. R.; Tack, T.; Bektesevic, S.; Abraham, M. A. *Catal. Commun.* **2003**, *4*, 309−314.
(21) Rathke, J. W.; Klinger, R. J.; Krause, T. R. *Organometallics* **1991**, *10*, 1350−1355.
(22) Palo, D. R.; Erkey, C. *Organometallics* **2000**, *19*, 81−86.
(23) Sellin, M. F.; Cole-Hamilton, D. J. *J. Chem. Soc., Dalton Trans.* **2000**, 1681−1683.
(24) Sellin, M. F.; Bach, I.; Webster, J. M.; Montilla, F.; Rosa, V.; Aviles, T.; Poliakoff, M.; Cole-Hamilton, D. J. *J. Chem. Soc., Dalton Trans.* **2002**, 4569−4576.
(25) Koch, D.; Leitner, W. *J. Am. Chem. Soc.* **1998**, *120*, 13398−13404.
(26) Bemi, L.; Clark, H. C.; Davies, J. A.; Fyfe, C. A.; Wasylishen, R. E. *J. Am. Chem. Soc.* **1982**, *104*, 438−445.
(27) Giordano, G.; Crabtree, R. H. *Inorg. Synth.* **1990**, *28*, 88−90.
(28) Komoroski, R. A.; Magistro, A. J.; Nicholas, P. P. *Inorg. Chem.* **1986**, *25*, 3917−3925.
(29) Baiker, A. *Chem. Rev.* **1999**, *99*, 453−473.

Received for review June 2, 2003. Revised manuscript received July 29, 2003. Accepted August 14, 2003.

ES034544N